Published in final edited form as:
Chem Res Toxicol. 2012 February 20; 25(2): 410–421. doi:10.1021/tx2004536.

Cytochrome P450-Mediated Metabolism and DNA Binding of 2-Amino-1,7-dimethylimidazo[4,5-*g*]quinoxaline and its Carcinogenic Isomer 2-Amino-3,8-dimethylimidazo[4,5-*f*]quinoxaline in Mice

Robert J. Turesky[†,*], **Erin E. Bessette**[†], **Deborah Dunbar**[†], **Rosa G. Liberman**[‡], and **Paul L. Skipper**[‡]

[†]Division of Environmental Health Sciences, Wadsworth Center, New York State Department of Health, Albany, New York 12201

[‡]Department of Biological Engineering, Massachusetts Institute of Technology, Cambridge, MA 02139

Abstract

2-Amino-1,7-dimethylimidazo[4,5-*g*]quinoxaline (MeI*g*Qx) is a recently discovered heterocyclic aromatic amine (HAA) that is formed during the cooking of meats. MeI*g*Qx is an isomer of 2-amino-3,8-dimethylmidazo[4,5-*f*]quinoxaline (MeIQx), a rodent carcinogen and possible human carcinogen that also occurs in cooked meats. MeI*g*Qx is a bacterial mutagen but knowledge about its metabolism and carcinogenic potential is lacking. Metabolism studies on MeI*g*Qx and MeIQx were conducted with human and mouse liver microsomes, and recombinant human P450s. DNA binding studies were also investigated in mice to ascertain the genotoxic potential of MeI*g*Qx in comparison to MeIQx. Both HAAs underwent comparable rates of *N*-oxidation to form genotoxic *N*-hydroxylated metabolites with mouse liver microsomes (0.2 - 0.3 nmol/min/mg protein). The rate of *N*-oxidation of MeIQx was 4-fold greater than the rate of *N*-oxidation of MeI*g*Qx with human liver microsomes (1.7 *vs* 0.4 nmol/min/mg protein). The rate of *N*-oxidation, by recombinant human P450 1A2, was comparable for both substrates (6 pmol/min/pmol P450 1A2). MeI*g*Qx also underwent *N*-oxidation by human P450s 1A1 and 1B1 at appreciable rates, whereas MeIQx was poorly metabolized by these P450s. The potential of MeI*g*Qx and MeIQx to form DNA adducts was assessed in female C57BL/6 mice given [^{14}C]-MeI*g*Qx (10 μCi, 9.68 mg/kg body wt) or [^{14}C]-MeIQx (10 μCi, 2.13 mg/kg body wt). DNA adduct formation in liver, pancreas and colorectum was measured by accelerator mass spectrometry at 4, 24 or 48 h post-treatment. Variable levels of adducts were detected in all organs. The adduct levels were similar for both HAAs, when adjusted for dose, and ranged from 1 to 600 adducts per 10^7 nucleotides per mg/kg dose. Thus, MeI*g*Qx undergoes metabolic activation and binds to DNA at levels that are comparable to MeIQx. Given the high amounts of MeI*g*Qx formed in cooked meats, further investigations are warranted to assess the carcinogenic potential of this HAA.

Introduction

More than 20 heterocyclic aromatic amines (HAAs) have been identified in cooked beef, poultry, and fish.[1,2] The formation of HAAs is dependent upon the type of meat and method

[*]Address correspondence to: Robert J. Turesky Phone: 518-474-4151 Fax: 518-473-2095, Rturesky@wadsworth.org.

Supporting Information Available: Additional information as noted in text (Figure S-1). This material is available free of charge via the Internet at http://pubs.acs.org.

of cooking: the concentrations of HAAs can range from less than 1 part-per-billion (ppb), up to 500 ppb in meat or poultry that is cooked well done.[2-4] The HAAs thus far assayed have been shown to induce tumors at multiple sites in rodents.[1] Several prevalent HAAs are classified as probable or possible human carcinogens (Group 2A and 2B), based on toxicity data reviewed by the International Agency for Research on Cancer.[5,6] The *Report on Carcinogens*, 11th edition, of the National Toxicology Program, also concluded that prevalent HAAs are "reasonably anticipated" to be human carcinogens.[7] Thus, there is much concern about the health risk associated with the exposure to these chemicals.

2-Amino-3,8-dimethylimidazo[4,5-*f*]quinoxaline (MeIQx) is one of the most abundant HAAs formed in cooked meats. MeIQx is a powerful bacterial mutagen and induces tumors at multiple sites in rodents during long-term feeding studies.[1] It is noteworthy that MeIQx and other known HAAs account for less than 30% of the mutagenicity attributed to this class of genotoxicants in well-done grilled meats and other uncharacterized HAAs are undoubtedly present.[8] We recently discovered 2-amino-1,7-dimethylimidazo[4,5-*g*]quinoxaline (MeI*g*Qx), a linear tricyclic ring isomer of MeIQx in urine of meat-eaters,[9] and subsequently identified MeI*g*Qx in cooked beef.[9-11] MeI*g*Qx is the most mass-abundant HAA formed in cooked ground beef, steaks and gravies;[4] it occurs at 5-fold or greater levels than the amounts of MeIQx or 2-amino-1-methyl-6-phenylimidazo[4,5-*b*]pyridine (PhIP). Both MeIQx and PhIP are believed to contribute to diet related cancers.[1] MeI*g*Qx is a less potent bacterial mutagen than MeIQx and PhIP; however, studies have not been conducted on the metabolism of MeI*g*Qx, and the carcinogenic potential of MeI*g*Qx is unknown.[11]

In this investigation, we have examined the capacities of human and mouse liver microsomes, and recombinant human cytochrome P450s to metabolize MeI*g*Qx and MeIQx to electrophilic metabolites that are capable of binding to DNA. We also compared the potential of [^{14}C]-MeI*g*Qx and [^{14}C]-MeIQx to bind to DNA in liver, pancreas and colorectum, potential target organs of HAA carcinogenicity, in C57BL/6 mice. These data provide a preliminary estimate of the genotoxic potential of MeI*g*Qx in vivo.

Materials and Methods

Chemicals

MeIQx and [2-^{14}C]-MeIQx (50 mCi/mmol, >98% radiochemical purity) were purchased from Toronto Research Chemicals (Ontario, Canada). KCN and Br_2 were was purchased from Sigma (St. Louis, MO). K[^{14}C]N (54 mCi/mmol) was purchased from Moravek Chemicals (Brea, CA). Human liver samples were from Tennessee Donor Services, Nashville, TN, and kindly provided by Dr. F.P. Guengerich, Vanderbilt University. Recombinant human P450s 1A1, 1A2 and 1B1 contained in supersomes from baculovirus-infected insect cells, and furafylline were purchased from Becton Dickinson (San Jose, CA).

General Methods

Mass spectra of synthetic derivatives and metabolites were acquired on a Finnigan TSQ Quantum Ultra triple stage quadrupole mass spectrometer (Thermo Fisher, San Jose, CA). The MS analyses were conducted in the positive ionization mode and employed an Advance CaptiveSpray™ source from Michrom Bioresource Inc. (Auburn, CA). Typical instrument tune parameters used were as follows: capillary temperature 200 °C, source spray voltage 1.4 kV, tube lens offset 95 V, capillary offset 35 V, and source fragmentation 5 V. Argon, set at 1.5 mTorr, was used as the collision gas and the collision energy was set between 15 to 30 eV; no sheath gas, sweep gas or auxiliary gas was employed.

Synthesis

The synthesis of [2-^{14}C]-MeI*g*Qx was done as previously described for the synthesis of the unlabelled compound with minor modifications.[11] K[^{14}C]N (0.093 mmol, 54 mCi/mmol) was diluted with KCN (0.4 mmol) in CH_3OH (0.6 mL), sonicated for 10 min, and then slowly added to Br_2 (0.50 mmol) in CH_3OH (0.5 mL) on ice. The reaction was allowed to proceed for 20 min. Thereafter, 4-fluoro-5-nitrobenzene-1,2-diamine (41 mg, 0.24 mmol) in C_2H_5OH (0.5 mL) was added to the newly formed [^{14}C]NBr, and the reagents were mixed overnight at room temperature. The 2-[^{14}C]-5-fluoro-6-nitro-1*H*-benzimidazole-2-amine intermediate was reacted with NH_4OH to displace the fluorine moiety, followed by reduction with $NaBH_4$, ring-closure with methylglyoxal, and lastly by methylation with CH_3I, as previously described.[11] [2-^{14}C]-MeI*g*Qx and its 6-methylated homologue were resolved by semi-preparative HPLC employing a Waters XBridge phenyl column (10 × 250 mm, 5 μm particle size). An isocratic solvent composed of 23% CH_3OH in 5 mM $NH_4CH_3CO_2$ (pH 8.7) was used for chromatography. The flow rate was 3 mL/min, and the run time was 70 min. The chemical and radiochemical purities of MeI*g*Qx exceeded 98.5% as judged by HPLC with UV diode array detection and liquid scintillation counting. The specific activity of MeI*g*Qx was determined by ESI-MS, by measuring the ratio of the $^{14}C/^{12}C$ isotopes of the protonated molecules $[M+H]^+$ at *m/z* 216.1 and 214.1: the specific activity was estimated at 11 mCi/mmol.

2-Hydroxyamino-3,8-dimethylimidazo[4,5-*f*]quinoxaline (HONH-MeIQx) was prepared by reduction of 2-nitro-3,8-dimethylimidazo[4,5-*f*]quinoxaline with hydrazine and Pd/C serving as a catalyst.[12] 2-Amino-8-(hydroxymethyl)-3-methylimidazo[4,5-*f*]quinoxaline (8-CH_2OH-IQx) was prepared by the oxidation of MeIQx with SeO_2 as previously described.[13] *N*-(deoxyguanosin-8-yl)-MeIQx (dG-C8-MeIQx), and [$^{13}C_{10}$]-dG-C8-MeIQx, and 5-(deoxyguanosin-N^2-yl)-MeIQx (dG-N^2-MeIQx) were synthesized by reaction of the *N*-acetoxy derivative of MeIQx with either dG or [$^{13}C_{10}$]-dG as previously reported.[14]

Microsomal metabolism studies

The metabolism studies were conducted with liver microsomes prepared from female C57BL/6J mice,[15] the mouse strain used for in vivo DNA binding studies, or with human liver microsomes, or recombinant human P450s 1A1, 1A2, and 1B1. Liver microsomal protein (1 mg/mL) or recombinant P450 (100 pmol/mL), in 100 mM potassium phosphate (pH 7.6) containing 0.5 mM EDTA, 5 mM glucose 6-phosphate, glucose 6-phosphate dehydrogenase (1 unit/mL), 1 mM NADPH, 1 mM NAD^+ were incubated with MeI*g*Qx or MeIQx (200 μM); the *N*-oxidation rates are at V_{max} for MeIQx at this substrate concentration.[15] The enzymes plus cofactors were incubated for 3 min prior to the addition of HAA substrates. The metabolism was done for 5 or 10 min, and metabolite formation was a linear function with time. Some metabolism studies with human liver microsomes were conducted for time periods up to 30 min, to produce large amounts of metabolites for characterization by mass spectrometry. The enzyme reactions were terminated by the addition of 2 vol CH_3OH. The precipitated proteins were removed by centrifugation and the supernatants were assayed by HPLC with an Agilent 1100 Chemstation equipped with an UV photodiode array detector. The metabolites were resolved with an Aquasil C18 column (4.6 × 250 mm, 5 μm particle size, Thermo Scientific), employing a linear gradient starting from 10% CH_3CN in 50 mM $NH_4CH_3CO_2$ (pH 6.8) and reaching 100% CH_3CN at 20 min at a flow rate of 1 mL/min.

The estimates of formation of 2-hydroxamino-1,7-dimethylimidazo[4,5-*g*]quinoxaline (HONH-MeI*g*Qx) and 2-hydroxyamino-3,8-dimethylimidazo[4,5-*f*]quinoxaline (HONH-MeIQx), and other oxidation products were determined by HPLC with UV detection. The metabolites of MeI*g*Qx were monitored at 370 or 390 nm and metabolites of MeIQx were

monitored at 274 nm. We assumed that the molar extinction coefficients of *N*-hydroxylated and ring-oxidized metabolites were the same values as the molar extinction coefficients of the parent compounds at their respective maximal absorbance wavelengths. The UV responses at these wavelengths were used to estimate rates of metabolite formation.

Liquid chromatography-electrospray ionization/mass spectrometry (LC-ESI/MS) characterization of metabolites

The *N*-oxidized and ring-oxidized metabolites were collected from the HPLC effluent and directly characterized by electrospray ionization tandem mass spectrometry (ESI/MS^2) with the triple stage quadrupole mass spectrometer. The metabolites were also characterized by ESI/MS^2 following reaction with nitrosobenzene (10 μg, in 0.1% HCO_2H in CH_3OH) at 50 °C for 1 h.

In Vivo DNA Binding Studies

DNA binding studies were conducted with female C57BL/6J mice (Taconic Farm, Albany, NY). Animals were housed in polycarbonate cages and allowed to acclimate for 1 week prior to commencement of the study.

Animal Dosing

Mice (20 g, N = 5 animals per time point) were dosed by gavage with ^{14}C-MeI*g*Qx (10 μCi, 9.68 mg/kg body wt) or ^{14}C-MeIQx (10 μCi, 2.13 mg/kg body wt) in a volume of 0.25 mL water. At T 4, 24, or 48 h, animals were sacrificed by asphyxiation with CO_2 gas, followed by cervical dislocation; blood was retrieved via the inferior vena cava. The liver and pancreas were harvested, rinsed with chilled PBS and snapped-frozen in liquid nitrogen. The colorectal tissue (ileo-cecal junction to the rectum) was retrieved, the fecal contents were removed, and the tissue segment was incubated with cold, freshly prepared EDTA buffer (phosphate-buffered saline containing 1.5 mM Na_2-EDTA, 6000 U sodium heparin, DTT (8 mg) and phenylmethanesufonyl fluoride (4 mg, 100 μl of 40 mg/mL DMSO, per 100 ml of buffer). After 20 min, the mucosal layer containing the colonocytes was retrieved by placing the intestine segment in a Petri dish and the loosened mucosal layer was displaced by gently scraping the outer intestinal segment with the edge of a glass slide to eject the colonocytes. The colonocytes were centrifuged at 3,000 g at 4 °C. Pelleted colonocytes were resuspended in EDTA buffer (2 mL) and centrifuged again. This washing procedure was repeated a third time and the colonocytes were quick-frozen in liquid nitrogen.

Radioactivity in plasma

Radioactivity was measured with a Beckman Coulter liquid scintillation counter (Fullerton, CA) with external calibration.

Isolation of DNA

The entire liver, pancreas, or colonocytes were homogenized in 2 mL TE Buffer (50 mM Tris-HCl, 10 mM EDTA, pH 8.0) and centrifuged for 10 min at 3,000 g. DNA was isolated from the nucelar pellets of the liver and kidney (equivalent of 200 mg tissue), and from the entire nuclear pellet of the colorectum, by solvent extraction as described by Gupta.[16] The purified DNA underwent a second solvent extraction procedure and ethanol precipitation step, to further remove non-covalently bound radioactivity.

The DNA was dissolved in distilled-deionized H_2O and the concentration was determined by UV spectroscopy, assuming a concentration of DNA (50 μg/mL) is equal to 1.0 absorbance unit at 260 nm. The A260:280 ratios were on average greater than 1.75.

Accelerator Mass Spectrometry

AMS analyses were conducted at the MIT BEAMS Lab using procedures described elsewhere in detail.[17] Sample aliquots (1.50 μL) were applied directly to a CuO matrix, and introduced into a laser-induced combustion interface for subsequent AMS analysis. Each run contained two quantitation standards ([^{14}C-methyl] bovine serum albumin, 0.003 dpm/μL), followed by two blanks (1 μg/μL human serum albumin), 10 samples, and another two standards. Quantitation was performed by integrating peaks produced in the continuous trace of ^{14}C detector count rate versus time generated during operation of the combustion interface, which produces and delivers the CO_2 of combustion to the AMS ion source, and taking the product of the sample/standard peak area ratio multiplied by the standard concentration as the concentration of the sample. Blank values, if measurable, were subtracted from the sample peak areas prior to calculating sample concentration.

DNA Adduct Measurements by LC-ESI/MS^3

DNA (100 μg) in 5 mM Bis-Tris-HCl buffer (pH 7.1, 50 μL) underwent enzymatic digestion with DNAse I for 1.5 h, followed by incubation with nuclease P1 for 3 h, and then digested with alkaline phosphatase and phosphodiesterase for 18 h.[18] These enzyme digestion conditions were shown to be highly efficient in the recovery of the dG-C8-MeIQx from calf thymus DNA modified with *N*-acetoxy-MeIQx.[14,19] The digest was added to 2 vol of chilled C_2H_5OH and placed on ice for 1 h, followed by centrifugation at 15,000 g to pellet salt and protein. The supernatants were transferred to silylated capillary LC vials and concentrated to dryness by vacuum centrifugation. The extracts were dissolved in 1:1 H_2O:DMSO (20 μL).

The adducts were separated from non-modified nucleosides with a NanoAcquity™ UPLC system (Waters Corporation, Milford, MA) interfaced with a linear quadrupole ion trap mass spectrometer (LTQ MS, Thermo Fisher, San Jose, CA). A Waters Symmetry trap column (180 μm x 20 mm, 5 μm particle size) was employed for online solid phase enrichment of the DNA adducts. The analytical column was a Michrom C18 AQ (0.3 × 150 mm, 3 μm particle size, Michrom Bioresources Inc., Auburn, CA). The DNA digests were injected onto the trap column and washed with 0.2% HCO_2H in 5% CH_3CN at a flow rate of 12 μL/min for 5 min. Thereafter, the DNA adducts were back-flushed onto the C18 AQ Michrom AQ column. A linear gradient was employed to resolve the DNA adducts, starting at 0.01% HCO_2H containing 5% CH_3CN and arriving at 0.01% HCO_2H in 95% CH_3CN at 20 min. The flow rate was set at 5 μL/min.

Mass spectrometric measurements were performed at the MS^3 scan stage in the positive ionization mode. The ion source was an Advance CaptiveSpray™ source from Michrom Bioresource Inc. (Auburn, CA). Representative optimized instrument tuning parameters were as follows: capillary temperature, 200 °C; source spray voltage, 2.0 kV; no sheath gas, sweep gas or auxiliary gas was employed; capillary voltage, 40 V; tube lens voltage, 110 V; and in-source fragmentation 10 V. The automatic gain control settings were full MS target 30000 and MS^n target 10000, and the maximum injection time was 10 ms. The MS/MS scan mode produced the aglycone ion BH^+_2 adducts $[M+H-116]^+$ or $[M+H-121]^+$ from the protonated dG-C8-MeIQx and dG-C8-[^{14}C]-MeIQx adducts or [$^{13}C_{10}$]dG-C8-MeIQx adduct, respectively. The ions monitored were as follows: dG-C8-MeIQx (*m/z* 479.1 > 363.1 >); dG-C8-[^{14}C]-MeIQx (m/z 481.1 > 365.1 >); and [$^{13}C_{10}$]-dG-C8--C8-MeIQx (*m/z* 489.1 > 368.1 >). The product ion spectra of the aglycone adducts at the MS^3 scan stage were acquired from *m/z* 125 to 400. The normalized collision energies were set at 24 and 34 eV, and the isolation widths were set at an *m/z* = 4.0 and 1.0, respectively, for the MS^2 and MS^3 scan modes. The activation Q was set at 0.35 and the activation time was 10 ms for both transitions. Helium was used as the collision damping gas in the ion trap and was set at

a pressure of 1 mTorr. One μscan was used for data acquisition. The same mass spectral parameters were employed to screen for putative dG-C8 adducts of MeI*g*Qx.

Results

Metabolism of MeIQx and MeIgQx with human and mouse liver microsomes and recombinant human P450s

HAAs undergo bioactivation by cytochrome P450-mediated *N*-oxidation of the exocyclic amine group, to form electrophilic *N*-hydroxy-HAA metabolites that covalently bind to DNA.[20-22] The liver is the most active organ in the metabolism of HAAs,[20-22] and P450 1A2 is the major hepatic P450 involved in the *N*-oxidation of most HAAs.[15,23,24] We previously characterized the principal oxidation products of MeIQx formed by rat and human liver microsomes, rat P450 1A2, and recombinant human P450 1A2.[15] In this study, we have examined the pathways of P450-mediated metabolism and compared the rates of *N*-oxidation of MeIQx and MeI*g*Qx, by employing microsomes prepared from liver of female CN 57/BL mice, the species used for in vivo DNA adduct binding studies. The capacities of human liver microsomes, recombinant human P450 1A2, P450 1A1, and P450 1B1 to bioactivate both compounds were also investigated. Both P450 1A1 and P450 1B1 are prominently expressed in extrahepatic tissues[25,26] and catalyze the *N*-oxidation of several HAAs.[27,28] The chemical structures of MeIQx and MeI*g*Qx and their proposed pathways of metabolism by human P450 1A2 (*vide infra*) are depicted in Figure 1.

The HPLC-UV profiles of the metabolites of MeIQx and MeI*g*Qx formed by human liver microsomes are shown in Figure 2, along with the UV spectra of the parent amines and their principal *N*-oxidized metabolites. The major pathway of metabolism of MeIQx occurs by *N*-oxidation of the exocyclic amine group, to form HONH-MeIQx. The UV spectrum of HONH-MeIQx is identical the spectra of the metabolite and synthetic derivative previously reported;[29] the absorbance maximum (272 nm) displays a slight hypsochromic shift relative to the absorbance maximum of MeIQx (274 nm) (Figure 2).[29] The dihydroxylated product, 2-(hydroxyamino)-8-hydroxymethyl-3-methylimidazo[4,5-*f*]quinoxaline (HONH-8-CH_2OH-IQx) is the second most abundant metabolite, followed by the alcohol, 8-CH_2OH-IQx, which is a minor metabolite.[30] Human liver microsomes also produced three oxidation products (M-1, M-2, and M-3) of MeI*g*Qx (Figure 2). Their UV and mass spectral data are discussed below.

The metabolites of MeIQx and MeI*g*Qx were collected from the HPLC effluent and directly infused into the triple stage quadrupole mass spectrometer. The product ion spectra of HONH-MeIQx and its azoxy derivative, obtained by reaction of HONH-MeIQx with nitrosobenzene, are shown in Figure 3. The product ion spectrum of HONH-MeIQx ([M +H]$^+$ at *m/z* 230.1) showed prominent fragment ions at *m/z* 213.1 and 212.1, indicative of the loss of 17 and 18 Da, which are attributed to loss of HO$^\cdot$ and H_2O. These fragment ions are typically observed in product ion spectra of HONH-HAA metabolites, but they are not present in the product ion spectra of ring-oxidized HAA metabolites, which often display a neutral loss of 28 Da (CO).[30,31] The product ion spectrum of the azoxy derivative confirms the structure as HONH-MeIQx.[29,32] The product ion spectra of HONH-8-CH_2OH-IQx and 8-CH_2OH-IQx (Figure 4) are also in excellent agreement to the spectra of the reference compounds previously reported.[30]

The mass spectrum of principal metabolite of MeI*g*Qx (M–3) displayed a protonated ion [M +H]$^+$ at *m/z* 230.1, a mass which is 16 Da greater than MeI*g*Qx. The ESI product ion spectra of M-3 and its adduction product with nitrosobenzene were very similar to the product ion spectra of HONH-MeIQx and its azoxy adduct (Figure 3). M-3 underwent oxidation with time, as did HONH-MeIQx, to form the presumed nitroso derivative: a prominent ion [M

+H]$^+$ was observed at *m/z* 228.1. The product ion spectra of these intermediates displayed prominent fragment ions at *m/z* 213.1 and 198.1, which are ascribed, respectively, to the loss of $CH_3^{\cdot}$ and NO moieties (data not shown). Thus, the structure of M-3 is assigned as 2-(hydroxamino)-1,7-dimethylimidazo[4,5-*f*]quinoxaline (HONH-MeI*g*Qx).

A large bathochromic shift was observed in the UV spectrum of HONH-MeI*g*Qx compared to the spectrum of MeI*g*Qx. The maximum of absorbance of M-3 was situated at 385 nm, whereas the maximum absorbance of MeI*g*Qx occurred at 365 nm (Figure 2). This large bathochromic shift is not observed in the UV spectrum of HONH-MeIQx, nor is this bathochromic shift observed in the UV spectra of the structurally related *N*-hydroxy-HAA derivatives of 2-amino-3-methylimidazo[4,5-*f*]quinoline or PhIP. However, the UV spectrum of the proposed *N*3-glucuronide conjugate of 2-(hydroxyamino)-1-methyl-6-phenylimidazo[4,5-*b*]pyridine (HONH-PhIP), which exists as an oxime, also displays a bathochromic shift of ~20 nm in its maximum absorbance in comparison to HOHN-PhIP.[31,33] We surmise that HONH-MeI*g*Qx exists preferentially as the oxime, and not as the *N*-hydroxylamine tautomer. The carcinogen 4-hydroxyamino quinoline 1-oxide was also reported to preferentially exist in its 4-hydroxyimino tautomeric form.[34]

The second most abundant metabolite of MeI*g*Qx (M-2) displayed a UV spectrum similar that of MeI*g*Qx. The mass spectrum of M-2 displayed a protonated ion at [M+H]$^+$ at *m/z* 230.0, indicative of another mono-oxidation metabolite. Prominent ions were observed in the product ion spectrum at *m/z* 201.0, 200.0, and 186.1 (Figure 4). These fragment ions are proposed to arise through losses of $HCO^{\bullet}$, H_2CO, and $HCO^{\bullet}$ + $CH_3^{\bullet}$. The product ion spectrum of M-2 is consistent with a ring-hydroxylated metabolite of MeI*g*Qx: the site of oxidation may have occurred at the C-4 or C-9 position of the quinoxaline skeleton (Figure 1). If oxidation had occurred at the 7-CH_3-group, a prominent fragment ion would have been expected at *m/z* 212.1 [M+H -18]$^+$, due to the loss of H_2O, as is observed in the product ion spectrum of 8-CH_2OH-IQx (Figure 4).

The third metabolite of MeI*g*Qx (M-1) displayed a UV spectrum that was very similar to spectrum of HONH-MeI*g*Qx (M-3), with a maximum absorbance situated at 385 nm. The full scan mass spectrum of M-1 displayed a protonated ion [M+H]$^+$ at *m/z* 246.1, indicating that the metabolite is a dihydroxylated product of MeI*g*Qx. Prominent ions are observed in the product ion spectrum at *m/z* 228.1 and 229.1, indicative of the loss of 17 and 18 Da and suggestive of the presence of the *N*-hydroxylamine moiety (Figure 4). The base peak, observed at *m/z* 200.1, is ascribed to the loss H_2O, followed by loss of CO. Thus, the product ion spectrum is consistent with the structure of a dihydroxlyated metabolite of MeI*g*Qx that contains the *N*-hydroxylamine moiety with the second site of hydroxylation possibly occurring at the C-4 or C-9 position of the quinoxaline ring.

8-CH_2OH-HONH-IQx and the dihydroxylated metabolite of MeI*g*Qx (M-1) were reacted with nitrosobenzene to form azoxy adducts. Protonated molecules [M+H]$^+$ were observed at *m/z* 335.2, a mass that is consistent with the molecular weight of the proposed azoxy conjugates (Figure S-1, Supporting Information). The product ion spectrum of the azoxy derivative of 8-CH_2OH-HONH-IQx displays prominent ions at *m/z* 317.1 and 299.3, which are ascribed to loss of one and two molecules of H_2O, whereas, the product ion spectrum of the azoxy derivative of M-1 displays prominent fragment ions at *m/z* 317.2 and 289.2, which are consistent with the loss of H_2O and H_2O+CO. These mass spectral data provide additional support for the secondary site of oxidation proposed to occur at the quinoxaline ring and not the 7-methyl group of MeI*g*Qx.

Estimated Rates of P450-Mediated Oxidation of MeIQx and MeI*g*Qx

The estimated rates of *N*- and C-oxidation of MeIQx and MeI*g*Qx, by mouse and human liver microsomes and recombinant human P450s, are summarized in Table 1. The *N*-oxidation rates of MeIgQx and MeIQx with mouse liver microsomes were comparable, whereas the rate of *N*-oxidation of MeIQx was about 4-fold higher than for MeI*g*Qx with human liver microsomes. MeI*g*Qx underwent *N*-oxidation by recombinant human P450 1A2, but also by extrahepatic P450s 1A1 and 1B1. Moreover, the rate of MeI*g*Qx *N*-oxidation of P450 1A1 was ~3-fold greater than the rate of *N*-oxidation carried out by P450 1A2. Human P450 1A2 appears to be involved only in *N*-oxidation (bioactivation), whereas P450 1A1 and P450 1B1 catalyze both *N*-oxidation and ring-oxidation (detoxication) of MeI*g*Qx. In contrast to MeI*g*Qx, the *N*-oxidation of MeIQx by P450s 1A1 and 1B1 was low to not detectable.

In Vivo DNA Binding Studies in Mice

Plasma Clearance

The study design was not intended to completely describe the rate of absorption and clearance profile of these chemicals. However, the data obtained from the 3 time points show that the kinetics of absorption and elimination of both ^{14}C-MeI*g*Qx and ^{14}C-MeIQx were rapid. The peak plasma levels in radioactivity associated with both compounds occurred at 4 h, and greater than 95% of the radioactivity was cleared from plasma within 48 h (Figure 5).

DNA Adducts

The apparent levels of [^{14}C]-MeI*g*Qx- and [^{14}C]-MeIQx-DNA adduct formation and removal in liver, pancreas and colorectal DNA are presented in Figure 6. The clearance of ^{14}C-isotope associated with DNA was less rapid than the clearance of ^{14}C-radioactivity associated with either carcinogen from plasma. The [^{14}C]-MeI*g*Qx isotope associated with liver DNA at T 24 and T 48 h was 33% and 27% of the ^{14}C-isotope detected at 4 h, whereas the isotope level associated to pancreas DNA was 44% and 17% of the level of ^{14}C-isotope bound to DNA at 4h. The [^{14}C]-MeIQx isotope associated with liver and pancreas DNA also appeared to persist: up to 74% and 25% of the ^{14}C-isotope observed in DNA of these organs at 4 h remained, respectively, at 48 h. The [^{14}C]-MeI*g*Qx isotope in colorectal DNA reached its maximum at 24 h, while the highest level of the [^{14}C]-MeIQx isotope in colorectal DNA was observed at 4 h. The disposition and elimination of MeI*g*Qx in the mouse is not known. The fecal content may contain high levels of ^{14}C isotope, resulting in high levels of exposure to this carcinogen, perhaps at greater levels than most other tissues.

LC-ESI/MS^3 of DNA Adducts

The formation of DNA adducts of [^{14}C]-MeIQx and [^{14}C]-MeI*g*Qx was examined by LC-ESI/MS^3 with a linear quadrupole ion trap mass spectrometer. The ion trap MS permits multi-stage tandem scanning for structural characterization and identification of the aglycone adducts $[BH_2]^+$.[18,35] Two isomeric dG adducts of MeIQx, dG-C8-MeIQx and dG-*N*^{2}-MeIQx are formed in vivo in liver of rats[19] and in human hepatocytes.[36] In addition, a third adduct is formed with dA; the structure has been tentatively assigned as 5-(deoxyadenosin-*N*^{6}-yl)-MeIQx (dA-*N*^{6}-MeIQx) (Figure 7).[37]

The stable isotope dilution method was used to measure the levels of dG-C8-MeIQx formed in mouse liver at the 24 h time point. Reconstructed ion chromatograms for dG-C8-MeIQx, dG-C8-[^{14}C]-MeIQx, [$^{13}C_{10}$]-dG-C8-MeIQx and a putative isomeric dG-C8-MeI*g*Qx at the MS^3 scan stage are presented in Figure 8. Both the dG-C8-MeIQx and dG-C8-[^{14}C]-MeIQx

adducts are observed. The product ion spectra of the unlabeled and labeled adducts, at the MS^3 scan stage, confirmed the structure of the adducts.[19,35]

The estimate of total [^{14}C]-MeIQx-DNA adduct formation in liver 24 h post treatment, based upon AMS measurements, was 11.4 ± 7.6 adducts per 10^8 nucleotides versus to 3.8 ± 0.6 dG-C8-MeIQx adducts per 10^8 nucleotides, based on quantitative LC-ESI/MS^3 measurements. The contribution of dG-C8-MeIQx to total ^{14}C bound to DNA ranged from 13 - 72% of the radioactivity. The relative response of the signals for dG-N^2-MeIQx and dA-N^6-MeIQx adducts, by LC-ESI/MS^3, are ~5% of the response of the signal observed for dG-C8-MeIQx.[37] The dG-N^2-MeIQx and dA-N^6-MeIQx adducts are formed in rat liver at levels that are respectively ~30 - 50% and ~5% of the level of dG-C8-MeIQx, 24 h following oral dosing with MeIQx (10 mg/kg).[19,37] If the relative level of formation of isomeric dG-MeIQx and dA-MeIQx adducts are similar in rat and mouse liver, the weak response in signals of dG-N^2-MeIQx and dA-N^6-MeIQx would preclude their detection, by LC-ESI/MS^3, in mouse liver DNA. Thus, the contribution of dG-N^2-MeIQx and dA-N^6-MeIQx adduct formation to the amount of [^{14}C]-MeIQx bound to DNA has not been taken into account, and the ^{14}C-isotope associated to the DNA as covalently bound adducts likely exceeds the contribution made by the dG-C8-MeIQx adduct. In a previous AMS study conducted with male C57BL/6 mice treated with [^{14}C]-MeIQx, the formation of liver adducts was shown to be linearly dependent on dose from an exposure of 5 mg down to 500 ng per kg of body weight).[38] The amount [^{14}C]-MeIQx bound to liver DNA was estimated at about 20 adducts per 10^8 nucleotides at 24 h post-treatment with [^{14}C]-MeIQx (5 mg/kg). This estimate in ^{14}C-adduct formation is remarkably similar to the level of [^{14}C]-MeIQx bound to liver DNA, when adjusted per dose, in our study.

In contrast to MeIQx, a putative dG-C8-Me*Ig*Qx adduct was not detected, when scanning at the MS^2 or MS^3 scan stages. The potential formation of a dA adduct of Me*Ig*Qx ($[M+H]^+$ at *m/z* 463.2) was also monitored, but no peaks were detected above background level. The data-dependent constant neutral loss-triple stage mass spectrometry scanning mode (CNL/MS^3) was employed to monitor for the loss of the deoxyribose moiety, followed by MS^3 of the putative aglycone adducts $[BH_2]^+$.[37] However, the CNL/MS^3 mode also failed to detect any adducts of Me*Ig*Qx.

Carcinogen Binding Index (CBI)

The CBI is a measure of the amount of adduct formed from a given dose; it is calculated by dividing the amount of adduct per unit of DNA by the dose per unit of body mass (μmol adduct bound per mole nucleotide)/(mmol chemical administered per kg animal).[39] The CBI of Me*Ig*Qx and MeIQx in liver, pancreas and colorectum are presented in Table 2. The CBI data are reported at the T 4, 24 and 48 h time points. The CBI values for liver DNA adduct formation of Me*Ig*Qx and MeIQx were not significantly different at T 4 and 24 h ($P > 0.4$, student's unpaired *t* test); however, the CBI values were significantly different at T 48 h ($P < 0.005$). These data are suggestive of a faster rate of apparent Me*Ig*Qx-DNA adduct removal than for MeIQx-DNA adducts in liver; additional time points are required to accurately determine the rate of adduct elimination. For extrahepatic tissues, there was a significant difference ($P < 0.01$) between MeIgQx and MeIQx CBI values of pancreas at 24 h and colorectal tissue at 48 h.

Discussion

This study was designed to examine the capacity of Me*Ig*Qx to undergo metabolic activation to form DNA adducts in comparison with its isomer, MeIQx, a multi-site carcinogen in rodents.[1] The metabolism and DNA binding data provide a preliminary assessment of the genotoxic potential of Me*Ig*Qx relative to MeIQx, which also induces *lacI* mutations in liver

and colon[40] and aberrant crypt foci in C57BL/6N mice,[41] the species employed for our DNA binding studies. The estimated rates of P450-mediated *N*-oxidation of MeI*g*Qx with mouse liver microsomes and the in vivo ^{14}C-binding data of MeI*g*Qx, when adjusted for dose, are comparable to those data obtained for MeIQx. We employed the highly sensitive AMS method for adduct detection,[17,38] which enabled us to estimate DNA adduct formation based upon ^{14}C isotope bound to DNA, since the structures of the MeI*g*Qx adducts are unknown.

MeIQx and other structurally related HAAs studied induce tumors at multiple sites in rodents during long-term feeding studies. The target organs include the oral cavity, liver, stomach, colon, pancreas, and the prostate gland in males, and the mammary gland in females.[1,42] The total dose required to induce tumor formation (TD_{50}) varies for each HAA and is host species-dependent. The TD_{50} values of the individual HAAs have been reported to range from 0.1 to 64.6 mg/kg/day in rodents.[1] MeIQx is a liver carcinogen in CDF_1 mice:[1] the TD_{50} value of MeIQx in this mouse strain is 24 mg/kg (http://potency.berkeley.edu/chempages/MeIQx.html).

The CBI approach has been used in rodent models as a means to assess the carcinogenic potential of genotoxic chemicals.[43] A CBI value of 1-10 is characteristic of weak carcinogens, while moderate carcinogens display CBI values of about 100.[39] The CBI for both MeIQx and MeI*g*Qx in liver were comparable at T4 and 24 h (CBI = 7 - 28). These findings suggest that MeI*g*Qx would be a weak to moderate liver carcinogen in this animal model. The [^{14}C]-MeI*g*Qx isotope is also associated with DNA in pancreas and colorectal tissue, suggesting that tumors could form in these organs as well. However, the presence of DNA adducts alone is insufficient to predict the development of cancer as carcinogenesis involves numerous biological events.[44] Moreover, dietary, environmental, and genetic factors can greatly impact the biological potency of HAAs and other genotoxicants.[1,45,46]

Thus far, we have not successfully identified MeI*g*Qx-DNA adducts by LC-ESI/MS^n. We surmise that the linear fused tricyclic ring structure of MeI*g*Qx inhibits the efficacy of enzymatic digestion of the MeI*g*Qx-adducted to DNA, and the MeI*g*Qx adducts may be present as incompletely digested oligomers, which escaped detection by LC-ESI/MS^n. Alternatively, the instrument tuning parameters of the mass spectrometer may not have been optimal for detection of MeI*g*Qx-DNA adducts, or the sensitivity in response of MeI*g*Qx-DNA adducts is at least 10-fold weaker than the signal of response for dG-C8-MeIQx. We have not been able to synthesize HONH-MeI*g*Qx by methods previously employed for the production of other HONH-HAAs.[12] Studies that examine the reactivity of synthetic HONH-MeI*g*Qx with deoxynucleosides and DNA are required to identify and elucidate the structures of MeI*g*Qx-DNA adducts.

HAAs have been classified as probable human carcinogens by IARC and by the National Toxicology Program, sponsored by NIEHS.[6,7] MeI*g*Qx is the most mass abundant HAA formed in cooked beef.[4,11] MeI*g*Qx is a bacterial mutagen; however its potency in the Ames reversion assay is about 4,000-fold lower than MeIQx, in *S. typhimurium* tester strain TA98. The genotoxic potency of MeI*g*Qx is 16-fold greater in *S. typhimurium* strain YG1024 than in *S. typhimurium* strain TA98. The YG1024 strain is derived from strain TA98 and contains high *O*-acetyltransferase activity that enhances the mutagenicity of some HAAs, presumably through the formation of reactive *N*-acetoxy intermediates, which covalently binds to DNA.[47] The higher potency of MeI*g*Qx in the YG1024 bacterial tester strain compared to TA98, indicates that the HONH-MeI*g*Qx undergoes *O*-acetylation to form the *N*-acetoxy intermediate, as does MeIQx.[11] MeI*g*Qx displays about 10-fold weaker mutagenic potency than the structurally related carcinogen PhIP (3,015 rev/μg) in *S. typhimurium* strain YG1024. It is noteworthy that the mutagenic potency of MeI*g*Qx is

comparable to the potency of 4-aminobiphenyl, a known human carcinogen, in TA98 and YG1024 (frameshift-specific) and YG1029 (primarily point mutation-specific) tester strains.[48-50] The strong mutagenic potencies of MeIQx and several other HAAs of angular tricyclic ring structure in the *S. typhimurium* TA98 strain have been attributed to the ability of these HAAs to frequently induce reversions about 9 base pairs upstream of the original CG deletion in the *his*D$^+$ gene in a run of GC repeats.[51] This sequence context may not be a hot-spot for MeI*g*Qx and PhIP adduct formation, or the capacities of MeI*g*Qx and PhIP adducts to induce mutations is weaker than the potencies of adducts formed by MeIQx and other angular tricyclic HAAs. The mutagenicity of MeI*g*Qx has not been assessed in mammalian cell systems. Such studies would provide additional data about the biological effects of MeI*g*Qx in comparison to carcinogenic HAAs, such as MeIQx and PhIP, and aid in assessing the health risk of this newly discovered HAA.

Both MeI*g*Qx and MeIQx undergo *N*-oxidation by mouse liver microsomes and by recombinant human P450 1A2 at similar rates. Moreover, recombinant human P450s 1A1 and 1B1, which are expressed in extrahepatic tissues,[25,26] are far more efficient at catalyzing the *N*-oxidation of MeI*g*Qx than the *N*-oxidation of MeIQx (Table 1). The differences in chemical structures of MeI*g*Qx and MeIQx appear to affect the regioselectivities of P450-mediated *N*-oxidation of the exocyclic amine groups, as well as the quinoxaline ring structures and methyl groups of both HAAs. The higher CBI values of putative MeI*g*Qx adducts formed in pancreas in comparison to MeIQx may be attributed to more efficient bioactivation of MeI*g*Qx by extrahepatic P450s.

Historically, short-term bacterial mutagenesis assays have been an effective screening tool for the identification of some mutagenic HAAs in complex food matrices, but they do not reliably predict carcinogenic potency in mammals.[52] MeI*g*Qx forms apparent DNA adducts at levels that are comparable to the levels of adducts formed by its carcinogenic isomer, MeIQx, when adjusted for dose. Given the elevated concentrations of MeI*g*Qx formed in cooked meats, further studies on the genetic toxicology and health risk of this novel HAA are clearly warranted.

Supplementary Material

Refer to Web version on PubMed Central for supplementary material.

Acknowledgments

Funding Source: This research was supported by grant R03ES016613 (E.E.B and R.J.T.) from the National Institute of Environmental Health Sciences, and by grant number 05B025 from the American Institute for Cancer Research (R.J.T.), and 2-PO1-ES006052 (R.L and P.L.S) from the National Institute of Environmental Health Sciences.

Abbreviations

AMS	accelerator mass spectrometry
CBI	carcinogen binding index
CNL/MS^3	constant neutral loss-triple stage mass spectrometry scanning mode
HAA	heterocyclic aromatic amine
LC-ESI/MS	Liquid chromatography-electrospray ionization/mass spectrometry
MeIgQx	2-amino-1,7-dimethylimidazo[4,5-*g*]quinoxaline

HONH-MeI*g*Qx	2-hydroxamino-1,7-dimethylimidazo[4,5-*g*]quinoxaline
MeIQx	2-amino-3,8-dimethylimidazo[4,5-*f*]quinoxaline
HONH-MeIQx	2-hydroxyamino-3,8-dimethylimidazo[4,5-*f*]quinoxaline
8-CH_2OH-IQx	2-amino-8-(hydroxymethyl)-3-methylimidazo[4,5-*f*]quinoxaline
HONH-8-CH_2OH-IQx	2-(hydroxyamino)-8-hydroxymethyl-3-methylimidazo[4,5-*f*]quinoxaline
PhIP	2-amino-1-methyl-6-phenylimidazo[4,5-*b*]pyridine
dG-C8-MeIQx	*N*-(deoxyguanosin-8-yl)-MeIQx, dG-N^2-MeIQx, 5-(deoxyguanosin-N^2-yl)-MeIQx
dA-N^6-MeIQx	5-(deoxyadenosin-N^6-yl)-MeIQx
ppb	part per billion

Reference List

1. Sugimura T, Wakabayashi K, Nakagama H, Nagao M. Heterocyclic amines: Mutagens/carcinogens produced during cooking of meat and fish. Cancer Sci. 2004; 95:290–299. [PubMed: 15072585]
2. Felton, JS.; Jagerstad, M.; Knize, MG.; Skog, K.; Wakabayashi, K. Contents in foods, beverages and tobacco. In: Nagao, M.; Sugimura, T., editors. Food Borne Carcinogens Heterocyclic Amines. John Wiley & Sons Ltd.; Chichester, England: 2000. p. 31-71.
3. Sinha R, Rothman N, Salmon CP, Knize MG, Brown ED, Swanson CA, Rhodes D, Rossi S, Felton JS, Levander OA. Heterocyclic amine content in beef cooked by different methods to varying degrees of doneness and gravy made from meat drippings. Food Chem. Toxicol. 1998; 36:279–287. [PubMed: 9651044]
4. Ni W, McNaughton L, LeMaster DM, Sinha R, Turesky RJ. Quantitation of 13 heterocyclic aromatic amines in cooked beef, pork, and chicken by liquid chromatography-electrospray ionization/tandem mass spectrometry. J. Agric. Food Chem. 2008; 56:68–78. [PubMed: 18069786]
5. International Agency for Research on Cancer. IARC Monographs on the Evaluation of Carcinogenic Risks to Humans: Tobacco smoking. International Agency for Research on Cancer; Lyon, France: 1986.
6. IARC Monographs on the Evaluation of Carcinogenic Risks to Humans. Some naturally occurring substances: food items and constituents, heterocyclic aromatic amines and mycotoxins. International Agency for Research on Cancer; Lyon, France: 1993.
7. National Toxicology Program. National Toxicology Program. Report on Carcinogenesis. Eleventh Edition. U.S. Department of Health and Human Services; Public Health Service, Research Triangle Park, N.C.: 2005.
8. Knize MG, Dolbeare FA, Carroll KL, Moore DH, Felton JS. Effect of cooking time and temperature on the heterocyclic amine content of fried beef patties. Food Chem. Toxicol. 1994; 32:595–603. [PubMed: 8045472]
9. Holland RD, Taylor J, Schoenbachler L, Jones RC, Freeman JP, Miller DW, Lake BG, Gooderham NJ, Turesky RJ. Rapid biomonitoring of heterocyclic aromatic amines in human urine by tandem solvent solid phase extraction liquid chromatography electrospray ionization mass spectrometry. Chem. Res. Toxicol. 2004; 17:1121–1136. [PubMed: 15310244]
10. Turesky RJ, Taylor J, Schnackenberg L, Freeman JP, Holland RD. Quantitation of carcinogenic heterocyclic aromatic amines and detection of novel heterocyclic aromatic amines in cooked meats and grill scrapings by HPLC/ESI-MS. J Agric. Food Chem. 2005; 53:3248–3258. [PubMed: 15826085]
11. Turesky RJ, Goodenough AK, Ni W, McNaughton L, LeMaster DM, Holland RD, Wu RW, Felton JS. Identification of 2-amino-1,7-dimethylimidazo[4,5-g]quinoxaline: an abundant mutagenic

heterocyclic aromatic amine formed in cooked beef. Chem Res. Toxicol. 2007; 20:520–530. [PubMed: 17316027]

12. Turesky RJ, Lang NP, Butler MA, Teitel CH, Kadlubar FF. Metabolic activation of carcinogenic heterocyclic aromatic amines by human liver and colon. Carcinogenesis. 1991; 12:1839–1845. [PubMed: 1934265]
13. Langouët S, Welti DH, Kerriguy N, Fay LB, Huynh-Ba T, Markovic J, Guengerich FP, Guillouzo A, Turesky RJ. Metabolism of 2-amino-3,8-dimethylimidazo[4,5-f]quinoxaline in human hepatocytes: 2-amino-3-methylimidazo[4,5-f]quinoxaline-8-carboxylic acid is a major detoxification pathway catalyzed by cytochrome P450 1A2. Chem. Res. Toxicol. 2001; 14:211–221. [PubMed: 11258970]
14. Turesky RJ, Rossi SC, Welti DH, Lay JO Jr. Kadlubar FF. Characterization of DNA adducts formed in vitro by reaction of N-hydroxy-2-amino-3-methylimidazo[4,5-f]quinoline and N-hydroxy-2-amino-3,8-dimethylimidazo[4,5-f]quinoxaline at the C-8 and N^2 atoms of guanine. Chem. Res. Toxicol. 1992; 5:479–490. [PubMed: 1391614]
15. Turesky RJ, Constable A, Richoz J, Varga N, Markovic J, Martin MV, Guengerich FP. Activation of heterocyclic aromatic amines by rat and human liver microsomes and by purified rat and human cytochrome P450 1A2. Chem. Res. Toxicol. 1998; 11:925–936. [PubMed: 9705755]
16. Gupta RC. ^{32}P-postlabelling analysis of bulky aromatic adducts. IARC Sci. Publ. 1993; 124:11–23. [PubMed: 8225473]
17. Liberman RG, Tannenbaum SR, Hughey BJ, Shefer RE, Klinkowstein RE, Prakash C, Harriman SP, Skipper PL. An interface for direct analysis of (14)C in nonvolatile samples by accelerator mass spectrometry. Anal. Chem. 2004; 76:328–334. [PubMed: 14719879]
18. Goodenough AK, Schut HA, Turesky RJ. Novel LC-ESI/MS/MS^n method for the characterization and quantification of 2′-deoxyguanosine adducts of the dietary carcinogen 2-amino-1-methyl-6-phenylimidazo[4,5-b]pyridine by 2-D linear quadrupole ion trap mass spectrometry. Chem. Res. Toxicol. 2007; 20:263–276. [PubMed: 17305409]
19. Paehler A, Richoz J, Soglia J, Vouros P, Turesky RJ. Analysis and quantification of DNA adducts of 2-amino-3,8-dimethylimidazo[4,5-f]quinoxaline in liver of rats by liquid chromatography/electrospray tandem mass spectrometry. Chem. Res. Toxicol. 2002; 15:551–561. [PubMed: 11952342]
20. Kato R, Yamazoe Y. Metabolic activation and covalent binding to nucleic acids of carcinogenic heterocyclic amines from cooked foods and amino acid pyrolysates. Jpn. J. Cancer Res. 1987; 78:297–311. [PubMed: 3108208]
21. Kato R. Metabolic activation of mutagenic heterocyclic aromatic amines from protein pyrolysates. CRC Crit. Rev. Toxicol. 1986; 16:307–348.
22. Turesky RJ. Interspecies metabolism of heterocyclic aromatic amines and the uncertainties in extrapolation of animal toxicity data for human risk assessment. Mol. Nutr. Food Res. 2005; 49:101–117. [PubMed: 15617087]
23. Butler MA, Iwasaki M, Guengerich FP, Kadlubar FF. Human cytochrome $P\text{-}450_{PA}$ (P450IA2), the phenacetin O-deethylase, is primarily responsible for the hepatic 3-demethylation of caffeine and N-oxidation of carcinogenic arylamines. Proc. Natl. Acad. Sci. U. S. A. 1989; 86:7696–7700. [PubMed: 2813353]
24. Guengerich FP, Turvy CG. Comparison of levels of several human microsomal cytochrome P-450 enzymes and epoxide hydrolase in normal and disease states using immunochemical analysis of surgical liver samples. J. Pharmacol. Exp. Ther. 1991; 256:1189–1194. [PubMed: 2005581]
25. Sutter TR, Tang YM, Hayes CL, Wo Y-YP, Jabs EW, Li X, Yin H, Cody CW, Greenlee WF. Complete cDNA sequence of a human dioxin-inducible mRNA identifies a new gene subfamily of cytochrome P450 that maps to chromosome 2*. J. Biol. Chem. 1994; 269:13092–13099. [PubMed: 8175734]
26. Ding X, Kaminsky LS. Human extrahepatic cytochromes P450: function in xenobiotic metabolism and tissue-selective chemical toxicity in the respiratory and gastrointestinal tracts. Annu. Rev. Pharmacol. Toxicol. 2003; 43:149–173. [PubMed: 12171978]

27. Hammons GJ, Milton D, Stepps K, Guengerich FP, Kadlubar FF. Metabolism of carcinogenic heterocyclic and aromatic amines by recombinant human cytochrome P450 enzymes. Carcinogenesis. 1997; 18:851–854. [PubMed: 9111224]

28. Crofts FG, Sutter TR, Strickland PT. Metabolism of 2-amino-1-methyl-6-phenylimidazo[4,5-b]pyridine by human cytochrome P4501A1, P4501A2 and P4501B1. Carcinogenesis. 1998; 19:1969–1973. [PubMed: 9855011]

29. Turesky RJ, Bracco-Hammer I, Markovic J, Richli U, Kappeler A-M, Welti DH. The contribution of N-oxidation to the metabolism of the food-borne carcinogen 2-amino-3,8-dimethylimidazo[4,5-f]quinoxaline in rat hepatocytes. Chem. Res. Toxicol. 1990; 3:524–535. [PubMed: 2103323]

30. Turesky RJ, Parisod V, Huynh-Ba T, Langouët S, Guengerich FP. Regioselective differences in C(8)- and N-oxidation of 2-amino-3,8-dimethylimidazo[4,5-f]quinoxaline by human and rat liver microsomes and cytochromes P450 1A2. Chem. Res. Toxicol. 2001; 14:901–911. [PubMed: 11453738]

31. Langouët S, Paehler A, Welti DH, Kerriguy N, Guillouzo A, Turesky RJ. Differential metabolism of 2-amino-1-methyl-6-phenylimidazo[4,5-b]pyridine in rat and human hepatocytes. Carcinogenesis. 2002; 23:115–122. [PubMed: 11756232]

32. Yamazoe Y, Abu-Zeid M, Manabe S, Toyama S, Kato R. Metabolic activation of a protein pyrolysate promutagen 2-amino-3,8-dimethylimidazo[4,5-f]quinoxaline by rat liver microsomes and purified cytochrome P-450. Carcinogenesis. 1988; 9:105–109. [PubMed: 3121205]

33. Kadlubar, FF.; Kaderlik, KR.; Mulder, GJ.; Lin, D-X.; Butler, MA.; Teitel, CH.; Minchin, RF.; Ilett, KF.; Friesen, MD.; Bartsch, H.; Nagao, M.; Esumi, E.; Sugimura, T.; Lang, NP. Metabolic activation and DNA adduct detection of PhIP in dogs, rats, and humans in relation to urinary bladder and colon carcinogenesis. In: Adamson, RH.; Gustafsson, J-A.; Ito, N.; Nagao, M.; Sugimura, T.; Wakabayashi, K.; Yamazoe, Y., editors. Heterocyclic Amines in Cooked Foods: Possible Human Carcinogens; 23rd Proceedings of the Princess Takamatusu Cancer Society; Princeton, NJ: Princeton Scientific Publishing Co., Inc.; 1995. p. 207-213.

34. Kawazoe Y, Ogawa O, Huang G-F. Studies on chemical carcinogens XVII: Structure of carcinogenic 4-hydroxaminoquinoline N-1 oxide derivatives. Tetrahedron. 1980; 36:2933–2938.

35. Bessette EE, Spivack SD, Goodenough AK, Wang T, Pinto S, Kadlubar FF, Turesky RJ. Identification of carcinogen DNA adducts in human saliva by linear quadrupole ion trap/multistage tandem mass spectrometry. Chem. Res. Toxicol. 2010; 23:1234–1244. [PubMed: 20443584]

36. Nauwelaers G, Bessette EE, Gu D, Tang Y, Rageul J, Fessard V, Yuan JM, Yu MC, Langouet S, Turesky RJ. DNA adduct formation of 4-aminobiphenyl and heterocyclic aromatic amines in human hepatocytes. Chem Res. Toxicol. 2011; 24:913–925. [PubMed: 21456541]

37. Bessette EE, Goodenough AK, Langouet S, Yasa I, Kozekov ID, Spivack SD, Turesky RJ. Screening for DNA adducts by data-dependent constant neutral loss-triple stage mass spectrometry with a linear quadrupole ion trap mass spectrometer. Anal. Chem. 2009; 81:809–819. [PubMed: 19086795]

38. Turteltaub KW, Felton JS, Gledhill BL, Vogel JS, Southon JR, Caffee MW, Finkel RC, Nelson DE, Proctor ID, Davis JC. Accelerator mass spectrometry in biomedical dosimetry: relationship between low-level exposure and covalent binding of heterocyclic amine carcinogens to DNA. Proc. Natl. Acad. Sci. U.S.A. 1990; 87:5288–5292. [PubMed: 2371271]

39. Lutz WK. In vivo covalent binding of organic chemicals to DNA as a quantitative indicator in the process of chemical carcinogenesis. Mutat. Res. 1979; 65:289–356. [PubMed: 390383]

40. Itoh1 T, Suzuki T, Nishikawa A, Furukawa F, Takahashi M, Xue W, Sofuni T, Hayashi M. In vivo genotoxicity of 2-amino-3,8-dimethylimidazo[4, 5-f]quinoxaline in lacI transgenic (Big Blue) mice. Mutat. Res. 2000; 468:19–25. [PubMed: 10863154]

41. Okonogi H, Ushijima T, Shimizu H, Sugimura T, Nagao M. Induction of aberrant crypt foci in C57BL/6N mice by 2-amino-9H-pyrido[2,3-b]indole (AalphaC) and 2-amino-3,8-dimethylimidazo[4,5-f]quinoxaline (MeIQx). Cancer Lett. 1997; 111:105–109. [PubMed: 9022134]

42. Shirai T, Sano M, Tamano S, Takahashi S, Hirose M, Futakuchi M, Hasegawa R, Imaida K, Matsumoto K, Wakabayashi K, Sugimura T, Ito N. The prostate: A target for carcinogenicity of 2-

amino-1-methyl-6-phenylimidazo[4,5-b]pyridine (PhIP) derived from cooked foods. Cancer Res. 1997; 57:195–198. [PubMed: 9000552]

43. Otteneder M, Lutz WK. Correlation of DNA adduct levels with tumor incidence: carcinogenic potency of DNA adducts. Mutat. Res. 1999; 424:237–247. [PubMed: 10064864]
44. Sugimura T. Multistep carcinogenesis: A 1992 perspective. Science. 1992; 258:603–607. [PubMed: 1411570]
45. Ghoshal A, Preisegger KH, Takayama S, Thorgeirsson SS, Snyderwine EG. Induction of mammary tumors in female Sprague-Dawley rats by the food-derived carcinogen 2-amino-1-methyl-6-phenylimidazo[4,5-b]pyridine and effect of dietary fat. Carcinogenesis. 1994; 15:2429–2433. [PubMed: 7955086]
46. Ubagai T, Ochiai M, Kawamori T, Imai H, Sugimura T, Nagao M, Nakagama H. Efficient induction of rat large intestinal tumors with a new spectrum of mutations by intermittent administration of 2-amino-1-methyl-6-phenylimidazo[4,5-b]pyridine in combination with a high fat diet. Carcinogenesis. 2002; 23:197–200. [PubMed: 11756241]
47. Schut HA, Snyderwine EG. DNA adducts of heterocyclic amine food mutagens: implications for mutagenesis and carcinogenesis. Carcinogenesis. 1999; 20:353–368. [PubMed: 10190547]
48. Scribner JD, Fisk SR, Scribner NK. Mechanisms of action of carcinogenic aromatic amines: an investigation using mutagenesis in bacteria. Chem.-Biol. Interact. 1979; 26:11–25. [PubMed: 380829]
49. Thompson PA, DeMarini DM, Kadlubar FF, McClure GY, Brooks LR, Green BL, Fares MY, Stone A, Josephy PD, Ambrosone CB. Evidence for the presence of mutagenic arylamines in human breast milk and DNA adducts in exfoliated breast ductal epithelial cells. Environ. Mol. Mutagen. 2002; 39:134–142. [PubMed: 11921181]
50. Radomski JL, Hearn WL, Radomski T, Moreno H, Scott WE. Isolation of the glucuronic acid conjugate of N-hydroxy-4-aminobiphenyl from dog urine and its mutagenic activity. Cancer Res. 1977; 37:1757–1762. [PubMed: 322861]
51. Fuscoe JC, Wu R, Shen NH, Healy SK, Felton JS. Base-change analysis of revertants of the hisD3052 allele in Salmonella typhimurium. Mutat. Res. 1988; 201:241–251. [PubMed: 3138534]
52. Sugimura T. Successful use of short-term tests for academic purposes: Their use in identification of new environmental carcinogens with possible risk for humans. Mutat. Res. 1988; 205:33–39. [PubMed: 3367922]

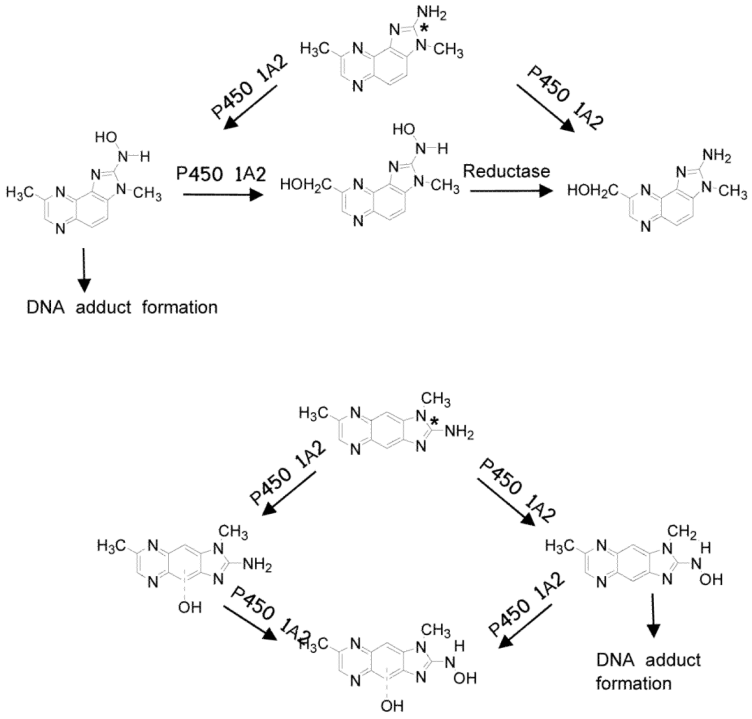

Figure 1.
Chemical structures of MeIQx and MeI*g*Qx and proposed pathways of P450-mediated metabolism. The * depicts the site of incorporation of the ^{14}C isotope.

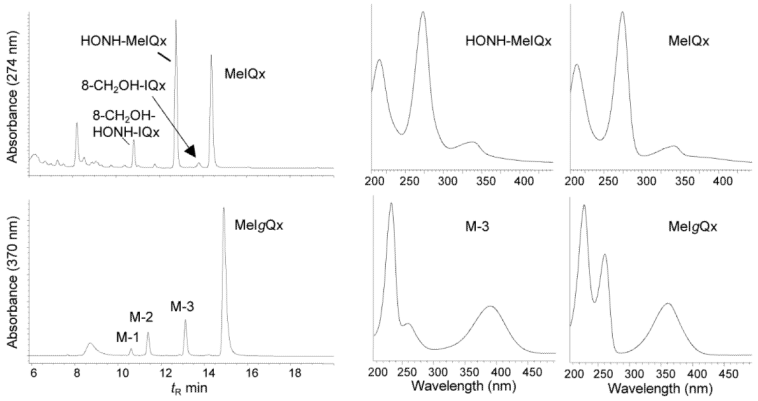

Figure 2.

HPLC UV profiles of MeIQx and MeI*g*Qx metabolites formed with human liver microsomes. The UV spectra of the parent compounds and major *N*-oxidized metabolites of each HAA are presented.

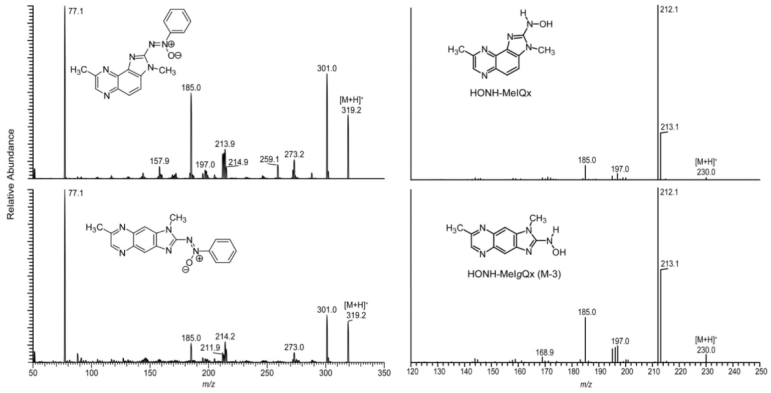

Figure 3.

The product ion spectra of HONH-MeIQx and HONH-MeIgQx (M-3) (right panel) and product ion spectra of the azoxy conjugates formed with nitrosobenzene (left panel).

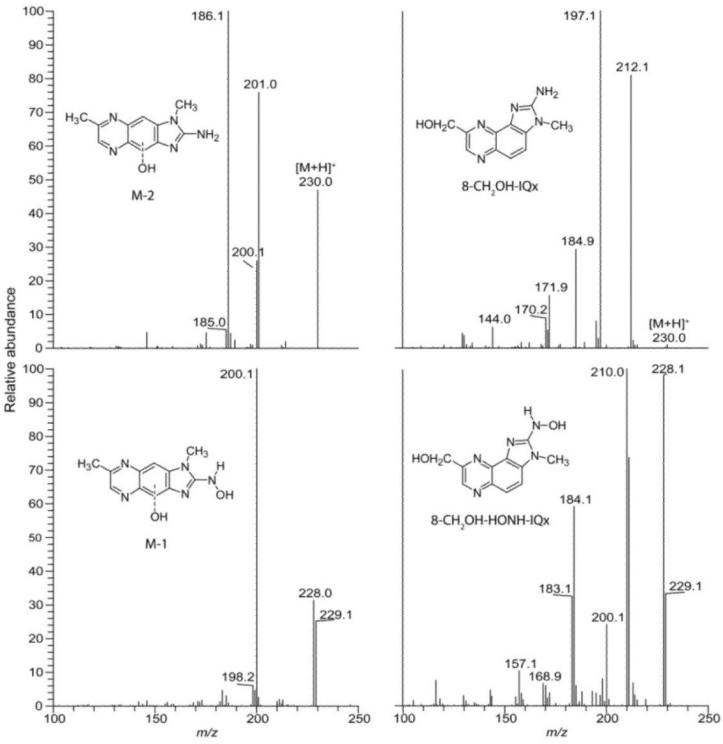

Figure 4.

ESI/MS/MS product ion spectra of 8-CH_2OH-IQx, 8-CH_2OH-HONH-IQx, and the monohydroxylated (M-2) and dihydroxylated (M-1) metabolites of MeI*g*Qx.

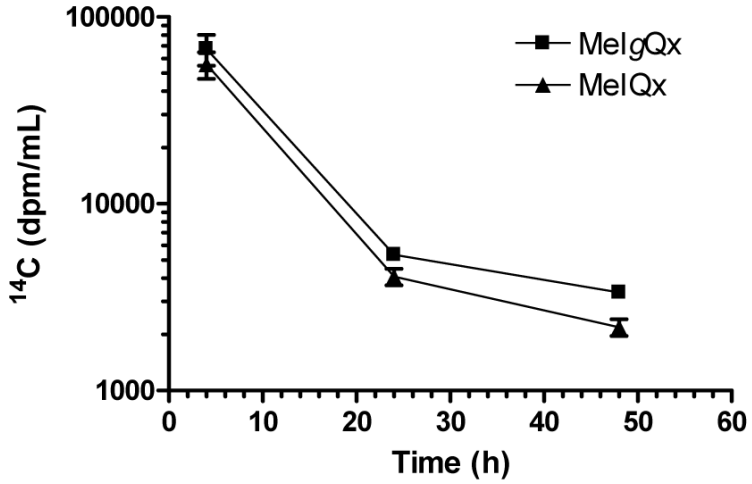

Figure 5.
Plasma clearance of [^{14}C]-MeIQx and [^{14}C]-MeI*g*Qx. Data represent the means and the standard deviations of 5 animals per time point.

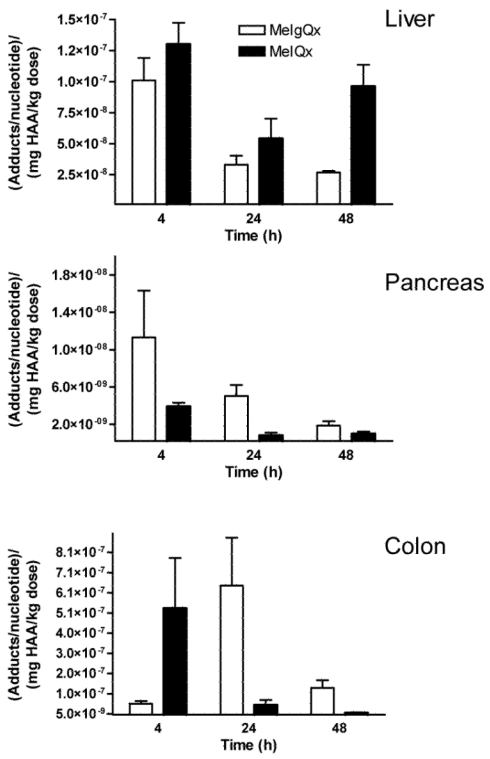

Figure 6.

The level of apparent [^{14}C]-MeIQx and [^{14}C]-MeI*g*Qx DNA adduct formation in liver, pancreas and colon as a function of time. Data represent the means and the standard error of the means of 5 animals per time point. The values of adduct formation were normalized to adducts per nucleotide/mg HAA/kg body weight .

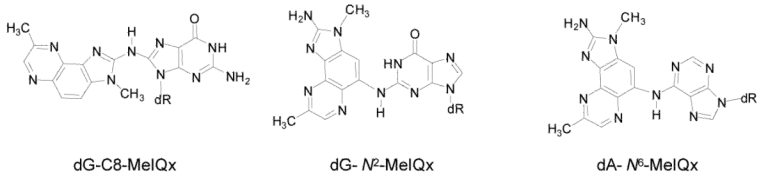

Figure 7.
Chemical structures of dG-C8-MeIQx, dG-N^2-MeIQx and dA-N^6-MeIQx

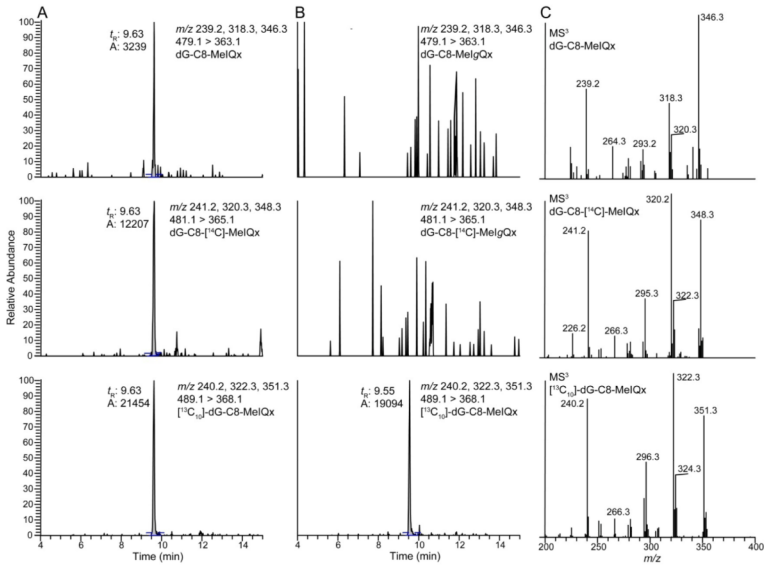

Figure 8.

Reconstructed ion chromatograms at the MS^3 scan stage for (A) dG-C8-MeIQx, dG-C8-[^{14}C]-MeIQx, and [$^{13}C_{10}$]-dG-C8-MeIQx, (B) putative dG-C8-MeI*g*Qx and dG-C8-[^{14}C]-MeI*g*Qx with [$^{13}C_{10}$]-dG-C8-MeIQx employed as an internal standard. The product ion spectra at the MS^3 scan stage of dG-C8-MeIQx, dG-C8-[^{14}C]-MeIQx and [$^{13}C_{10}$]-dG-C8-MeIQx are depicted in panel C.

Table 1

Estimated N-Oxidation and C-oxidation rates of MeIg Qx and MelQx with liver microsomes or recombinant human P450s

	nmol/min/mg microsomal protein or 100 pmol P450					
Enzyme	**HONH-MeI*g* Qx**	**HO-MeI*g* Qx**	**HONH-(HO)-MeIg Qx**	**HONH-MeIQx**	**HONH-8-CH_2OH-IQx**	**8-CH_2OH-IQx**
Mouse liver microsomes	0.3 ± 0.1	0.5 ± 0.2	ND	0.2 ± 0.01	ND	ND
Human liver microsomes	0.4 ± 0.02	0.1 ± 0.01	ND	1.7 ± 0.2	0.09 ± 0.01	ND
Recombinant human P450 1A1	14.1 ± 4.9	6.9 ± 2.4	ND	0.3 ± 0.1	ND	ND
Recombinant human P450 1A2	5.4 ± 2.1	ND	ND	6.1 ± 0.9	1.7 ± 0.5	ND
Recombinant human P450 1B1	3.9 ± 0.6	2.5 ± 0.3	ND	ND	ND	ND

Substrate = 200 μ M; Mean ± SD, N = 3 or 4 independent measurements

ND = not detected (< 0.05 nmol/min/mg protein or <0.05 nmol/min/100 pmol P450)

Table 2

Covalent Binding Index of MeIQx and MeIg Qx

	Liver: (μ mol/mol dNp)/(mmol carcinogen/kg bw)	
Time	**MeIgQx**	**MeIQx**
4	21.7 ± 8.6	27.7 ± 8.3
24	7.0 ± 3.2	11.5 ± 7.7
48	5.8 ± 0.6	20.5 ± 8.4
	Pancreas: (μ mol/mol dNp)/(mmol carcinogen/kg bw)	
Time	MeIgQx	MeIQx
4	2.4 ± 2.4	0.8 ± 0.2
24	1.1 ± 0.6	0.2 ± 0.1
48	0.2 ± 0.2	0.1 ± 0.1
	Colon: (μ mol/mol dNp)/(mmol carcinogen/kg bw)	
Time	MeIgQx	MeIQx
4	12.0 ± 6.5	113 ±119
24	138 ±114	10.4 ± 11.9
48	28.7 ± 18.5	2.1 ± 0.9

The mean ± SD of 4 or 5 animals per time point